

Stimuli-Responsive Self-Immolative Polymer Nanofiber Membranes Formed by Coaxial Electrospinning

Daewoo Han,[†] Xinjun Yu,^{‡, ID} Qinyuan Chai,[‡] Neil Ayres,[‡] and Andrew J. Steckl^{*,†, ID}

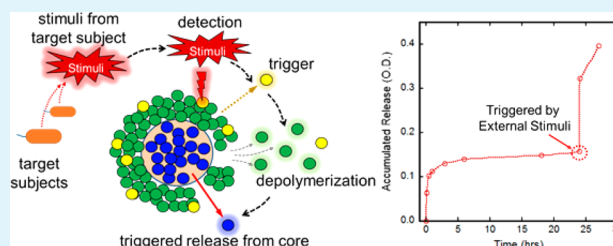
[†]Nanoelectronics Laboratory, Department of Electrical Engineering and Computing Systems, University of Cincinnati, Cincinnati, Ohio 45221, United States

[‡]Department of Chemistry, University of Cincinnati, Cincinnati, Ohio 45221, United States

S Supporting Information

ABSTRACT: The first self-immolative polymer (SIP) nanofiber membrane is demonstrated in this report, in which the immolation can be triggered by external stimulus. Electrospun SIP/polyacrylonitrile (PAN) fibers provide depolymerization that is ~25 times quicker and more responsive (i.e., immolation) than that of a cast film in the triggering condition. Depolymerization of SIP in the SIP/PAN blended fiber membrane results in the transition of the surface properties from hydrophobic (~110°) to hygroscopic (~0°). Triggered release of encapsulated functional molecules was demonstrated using coaxially electrospun fiber membrane made of a SIP/PAN blend sheath and polyvinylpyrrolidone/dye core. Coaxial fibers with the SIP/PAN sheath provide minimal release of the encapsulated material in nontriggering solution, while it releases the encapsulated material instantly when the triggering condition is met. Its versatility has been strengthened compared to that of non-SIP coaxial fibers that provide no triggering reaction by external stimulus.

KEYWORDS: coaxial electrospinning, self-immolative polymer, stimuli-responsive polymer, nanofiber, triggered release



INTRODUCTION

Stimuli-responsive polymers (SRP) represent an exciting research topic due to their unique ability to change their properties in response to external stimuli.^{1–3} Recently, a new type of stimuli-responsive polymer pioneered by the Shabat group, self-immolative polymers (SIPs),⁴ has gained attention as they afford a head-to-tail depolymerization upon being triggered by external stimuli.^{5–7} SIPs have been used to amplify a specific signal by releasing multiple detection molecules (attached to each monomer of the SIP) upon an external stimulus.^{8–10} More recently, a different approach has been investigated that uses SIPs as a sacrificial layer to contain functional molecules such as drugs and self-healing components, whose release is triggered only when targeted conditions are present.^{11–14}

Previously, Esser-Kahn et al. reported core-shell microcapsules bearing Boc and Fmoc triggering groups that can release encapsulated contents only under the removal conditions of each triggering group.¹¹ Similarly, DiLauro et al. demonstrated core-shell microcapsules that can be completely depolymerized in the presence of fluoride ions.¹² Another interesting SIP was reported by Fan et al., who developed an SIP using a commercially available monomer that provided a nontoxic byproduct after depolymerization.¹³ This approach gives the promise that SIPs can be synthesized conveniently and used as a versatile material for biomedical applications.^{13,14}

To date, SIP carriers for encapsulating materials have been developed in the form of microcapsules. Here, we report the

first SIP nanofibers formed by single and coaxial (core–sheath) electrospinning and the characterization of their triggered release behavior.

Electrospinning has developed into a versatile technique for producing free-standing nanofibrous membranes.^{15–17} The formation mechanism is straightforward and provides control over fiber morphology and material composition. Electrospun nanofiber membranes have an extremely high surface area with a highly porous network, which is greatly beneficial for many applications. This versatility can be further expanded by coaxial (core–sheath) and triaxial (core–intermediate–sheath) electrospinning that can produce multilayer structured nanofibers in a single step.^{18–23} Coaxial electrospinning enables the combination of different properties from each layer into single fiber, encapsulation and protection of functional molecules, and the controlled release of these functional molecules.

Generally, the complete depolymerization of SIP monoliths requires a fairly long time, ranging from a few hours to a few days.^{24,25} However, due to the extremely high surface area and porosity of nanofiber membranes, SIPs in the form of nanofiber membranes are expected to display very responsive and faster depolymerization in response to external stimuli.

The concept of combining coaxial fibers with a stimuli-responsive SIP is illustrated in Figure 1. This approach can provide on-demand (“triggered”) release of components

Received: December 22, 2016

Accepted: March 6, 2017

Published: March 6, 2017

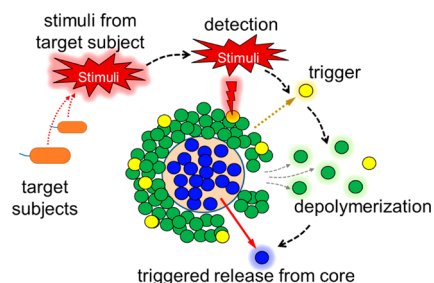


Figure 1. Basic concept diagram: cross section of coaxial fiber with self-immolative sheath and encapsulated core material. (Yellow circle, head molecules of SIP; green circle, SIP monomers; blue circle, encapsulated molecules).

embedded within the fibers. Once the trigger molecule is cleaved by external stimuli (such as enzymes,^{26,27} pH,^{28,29} UV light^{13,30}), head-to-tail depolymerization of the SIP layer occurs, enabling the release of functional molecules (such as drugs) from the underlying the core material. In the coaxial core–sheath structure, encapsulated material will be released rapidly upon triggering depolymerization because there is no barrier between the core material and the outer environment after SIP depolymerization.

EXPERIMENTAL SECTION

Materials. 4-Aminobenzyl alcohol, phenyl chloroformate, *tert*-butanol, tetrahydrofuran (THF), dibutyltin dilaurate (DBTL), sodium bicarbonate, anhydrous dimethylformamide (DMF), polyacrylonitrile (PAN, $M_w = 150$ kDa), poly(ϵ -caprolactone) (PCL, $M_n = 80$ kDa) and two different polyvinylpyrrolidone with a different molecular weight (M_w) of 360 kDa (PVP360) or 40 kDa (PVP40) were purchased from Sigma-Aldrich (St. Louis, MO). Dimethylformamide (DMF, 99.9% purity), 2,2,2-trifluoroethanol (TFE, 99.8% purity), trifluoroacetic acid (TFA), and dichloromethane (DCM) solvents were purchased from Fisher Scientific (Pittsburgh, PA). Rhodamine 640 perchlorate (RP) and Keyacid blue (KAB) dyes were purchased from Exciton (Dayton, OH) and Keystone (Chicago, IL), respectively. All materials were used as received without any further modification. ^1H and ^{13}C NMR measurements were performed in CDCl_3 with $\text{Si}(\text{CH}_3)_4$ as a reference using a 400 MHz Bruker Ultrashield (100 MHz for ^{13}C). ^1H NMR and ^{13}C NMR spectra were analyzed with MestReNova software. Molecular weights of polymers were determined using an Agilent 1100 Series HPLC equipped with DMF containing 0.1% LiBr as mobile phase and an Optilab rEX differential refractometer (light source = 658 nm) (Wyatt Technology Corporation) detector calibrated against poly(methyl methacrylate) standards (850–2 000 000 Da).

Synthesis of Phenyl (4-(Hydroxymethyl)phenyl)carbamate.

The monomer was synthesized according to a procedure from the literature.^{4,11} 4-Aminobenzyl alcohol (4.00 g, 32.5 mmol) was suspended in a 60 mL mixture of 2:2:1 of THF:saturated sodium bicarbonate (sat. NaHCO_3):water (volume ratio), and phenylchloroformate (4.16 mL, 33.1 mmol) was added dropwise over 5 min. The reaction proceeded at room temperature overnight. After this time, ethyl acetate was added, and the organic phase was washed twice with saturated NH_4Cl solution. The solvents were removed by rotary evaporation, and the crude product further purified by column chromatography on silica gel (30:70 ethyl acetate:hexane as mobile phase), yielding the desired product as a white solid (6.69 g, 85%). This product was identified by spectral comparison with literature data.² ^1H NMR (400 MHz, d_6 -DMSO): δ (ppm) 10.20 (1H, s), 7.45 (4H, m), 7.19 (5H, m), 5.07 (1H, t, $J = 5.6$ Hz), 4.43 (2H, d, $J = 5.6$ Hz).

Synthesis of Self-Immolative Polymer. Phenyl (4-(hydroxymethyl)phenyl)carbamate (4.00 g, 16.4 mmol) and DBTL (0.49 mL, 0.82 mmol) were added via a syringe to dry DMF (8 mL) in a Schlenk tube, which was preheated to 110 °C under an N_2 atmosphere. The reaction mixture was stirred for 15 min, after which *t*-butanol (7.77 mL, 81.2 mmol) in 8 mL of DMF was then added. The reaction mixture was stirred for an additional 30 min and was then allowed to cool to room temperature. The polymer was precipitated from cold methanol, filtered, and dried under vacuum. Polymer was obtained as a yellow powder (3.00 g, 75%). ^1H NMR (400 MHz, d_6 -DMSO): δ (ppm) 1.24 (9H, s), 5.06 (112H, s), 7.33(112H, d), 7.47(112H, d), 9.81 (52H, s). $M_n = 13$ kDa, dispersity (D) = 3.2.

Sample Preparation. For SIP-only electrospinning, the pure SIP solution was prepared by dissolving 25 wt% of SIP into DMF solvent, and the SIP/PAN blend solution was prepared by dissolving 7 wt % of SIP and 7 wt % of PAN in DMF solvent. For coaxial electrospinning, two solutions were prepared for core and sheath, respectively. The core solution consisted of 10 wt% PVP and 0.5 wt % of KAB dye in DMF solvent, while the same sheath solution with that of PAN/SIP 1:1 blend was used. Detailed sample descriptions, including electrospinning parameters, are shown in Table 1.

The cast sample was prepared by dispensing 100 μL of the same SIP/PAN blend solution on a flat aluminum foil. The dispensed solution was then dried overnight in ambient conditions. Thin film samples were prepared using a conventional spin-coating method. For contact angle measurements, PAN thin film was prepared by placing 300 μL of PAN (1 wt %) in DMF solution on 1" \times 1" glass substrates and then spinning them at 500 rpm for 30 s and 3000 rpm for 1 min. The same spin conditions were used for both SIP and SIP/PAN thin films using the SIP 2 wt% in DMF solution and the SIP 1 wt% + PAN 1 wt% in DMF solution, respectively. However, for the depolymerization experiment, SIP/PAN thin film samples were prepared by placing

Table 1. Sample Description with Electrospinning Parameters

solution	distance (cm)	voltage (kV)	flow rate (mL/h)	T (°C)	RH (%)	comment		
SIP 25 wt% in DMF	20	14	0.4	20.9	22	SIP-only		
PAN 7 wt% + SIP 7 wt% in DMF	20	13–14	0.8	21.1	34	SIP/PAN blend		
PAN 11 wt% in DMF	20	14.5–15	0.8	20.1	32	PAN-only		
core solution	sheath solution	distance (cm)	voltage (kV)	flow rate (mL/h)		T (°C)	RH (%)	comment
PVP360 15 wt% + RP dye 0.1 wt% in DMF	SIP 7 wt% + PAN 7 wt% in DMF	20	12.5	core	sheath	21.9	21	coaxial with SIP/PAN sheath
PVP360 10 wt% + KAB 0.5 wt% in DMF	SIP 7 wt% + PAN 7 wt% in DMF	20	12	0.2	0.8	20.3	23	coaxial with SIP/PAN sheath
PVP360 10 wt% + KAB 0.5 wt% in DMF	PAN 10 wt% in DMF	20	15	0.15	0.6	21.1	31	coaxial with PAN sheath
PVP360 4 wt% + PVP40 6 wt% + KAB 0.5 wt% in TFE	PCL 10 wt% in TFE	20	12.5	0.25	1.0	21.1	31	coaxial with PCL sheath

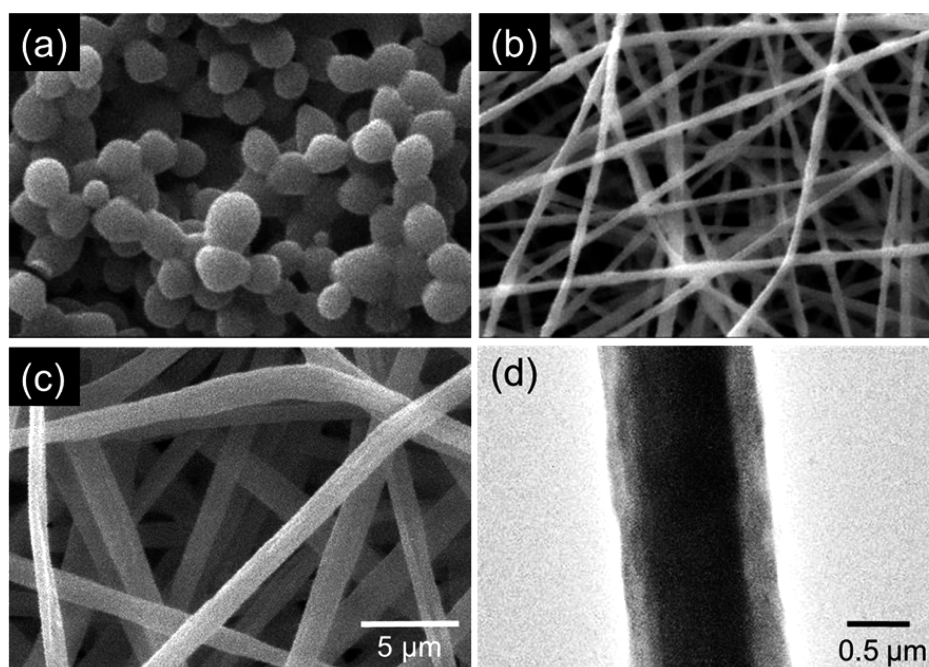


Figure 2. Electrospun SIP fiber morphologies: (a) electrospayed SIP microparticles; (b) single-nozzle blended electrospun SIP/PAN (1:1 wt. ratio) fibers; (c) coaxial fibers with SIP/PAN (1:1 wt. ratio) sheath and PVP/RP dye core; and (d) TEM observation of a single coaxial fiber. All SEM photos were taken at same scale.

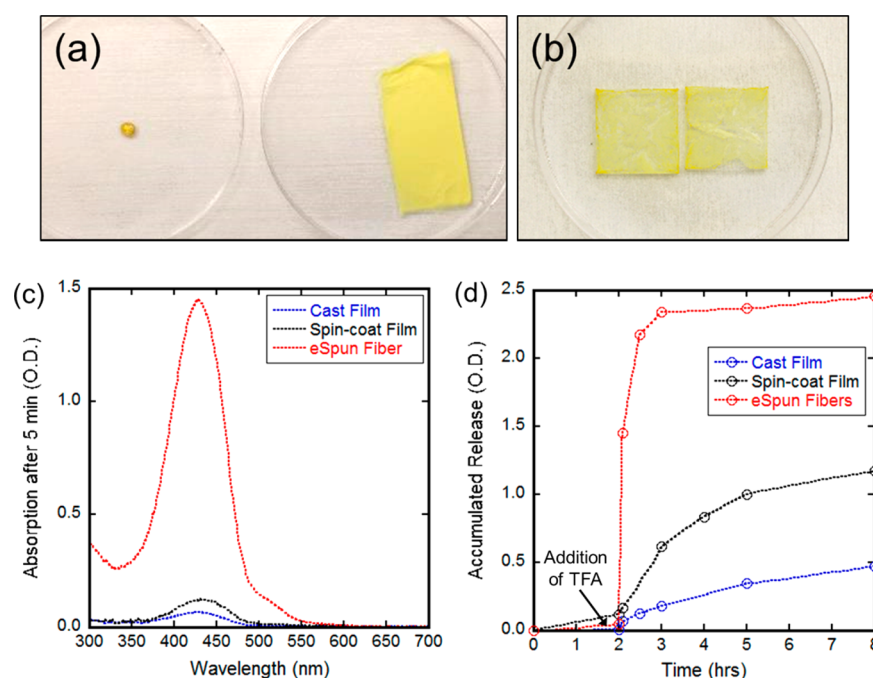


Figure 3. Depolymerization of SIP fiber membrane vs cast film: (a) 9 mg SIP/PAN samples of cast film (left) and electrospun membrane (right); (b) spin-coated SIP/PAN thin film sample with the same apparent area and material amount with the electrospun membrane; (c) optical absorption spectrum of the depolymerized/released SIP in solution 5 min after TFA addition in DCM solvent; and (d) release profile of depolymerized SIP from SIP/PAN fiber membranes.

800 μL of SIP 7 wt% + PAN 7 wt% in DMF solution on two 1" \times 1" glass slides and then spinning them at 500 rpm for 30 s and 1000 rpm for 1 min.

Triggering Release Experiments. Prepared SIP nanofiber membranes were immersed into various solvent mixtures with different TFA concentrations. TFA:DCM mixture was prepared in the volume ratio of 1:20, and TFA:DI mixtures were prepared in various volume ratios from 1:10 to 4:6. Once immersed, all samples

were agitated using a rotating agitator at the speed of 20 rpm. To quantify the amount of released components, UV-vis spectroscopy (PerkinElmer) was used to measure the absorption spectrum at multiple predetermined times after sample immersion.

Microscopy Methods. EVEX SX-30 mini-SEM was used to observe the fiber surface morphologies. Because all samples were insulating, a thin gold layer (<10 nm) was sputtered on the sample surface using a Denton Desk II instrument. The coaxial structure was

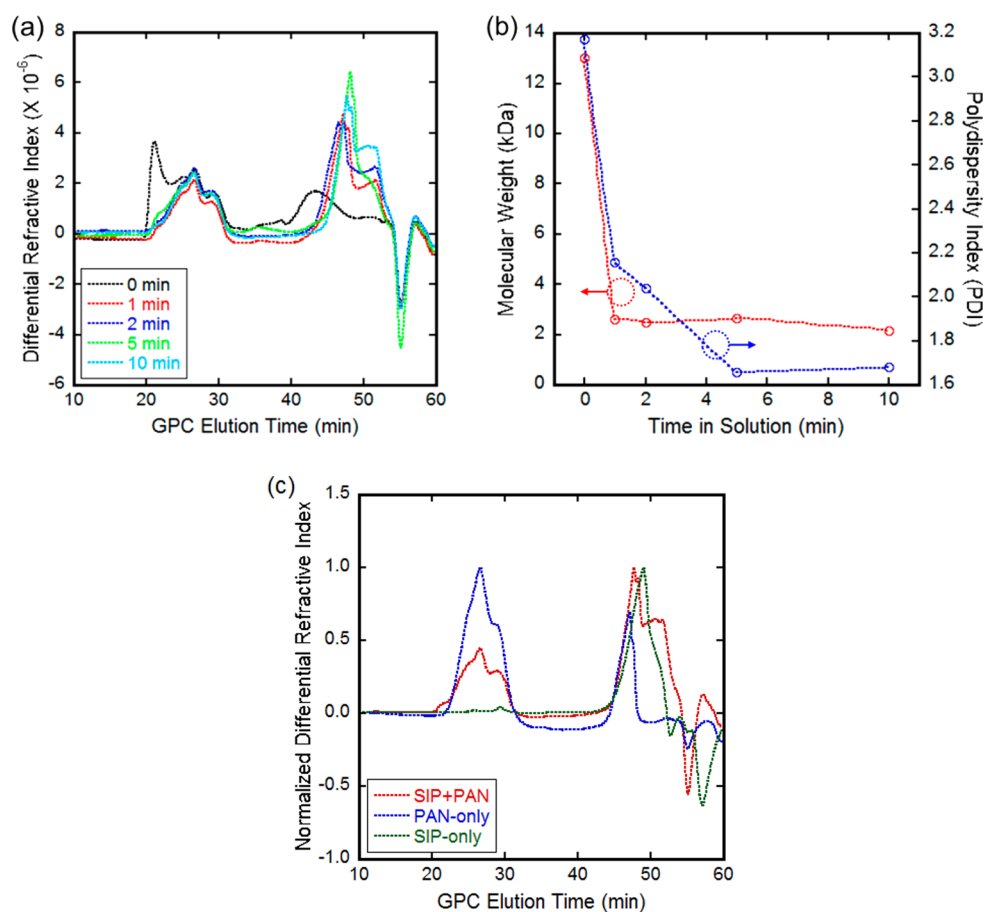


Figure 4. Molecular weight changes of PAN/SIP fiber membranes in TFA:DCM (1:20 vol ratio) solution obtained from GPC: (a) solution DRI vs GPC elution time for different solution soak times; (b) M_n and PDI change of SIP over depolymerization time; and (c) GPC data for SIP-only, PAN-only, and SIP + PAN composite fibers after 10 min solution soak time.

observed using an FEI CM20 transmission electron microscope (TEM). Fibers were directly electrospun on a copper TEM grid and observed at 200 kV acceleration voltage in the TEM.

RESULTS AND DISCUSSION

Because of the low molecular weight of SIPs, SIP solutions tend to have low viscosity. When the SIP-only solution was used for electrospinning, the ejected liquid jet quickly broke up due to the low viscosity of the solution even at >25 wt % of SIP in DMF and operated in the electrospinning mode, generating microbeads on the collector, as shown in Figure 2a. To increase the solution viscosity, the host polymer PAN ($M_w \sim 150$ kDa) was added to the SIP solution at 1:1 wt ratio with 7 wt % of each polymer in DMF. A SIP nanofiber mat prepared by electrospinning this blend solution is shown in Figure 2b. Although some phase separation between SIP and PAN was observed after mixing, the separation rate is sufficiently slow to allow the formation of homogeneous electrospun fibers. Moreover, coaxial fibers made of SIP/PAN sheath and PVP/dye core (Figure 2c) have been demonstrated, which can provide a triggered release of encapsulated functional materials from the core. In Figure 2d, the core–sheath structure of a single SIP coaxial fiber is observed, obtained by TEM at 200 kV acceleration voltage.

Differential scanning calorimetry (DSC)/thermogravimetric analysis (TGA) and Fourier transform infrared (FTIR) measurements were done to investigate the interaction between SIP and PAN polymers. In the DSC analysis (Figure S1a), we

could not detect the glass transition temperature (T_g) due to an unstable temperature ramp up to ~ 150 °C. Interestingly, thermal properties of the SIP/PAN blend show similarities to the PAN polymer rather than the SIP material. In the TGA measurements (Figure S1b), two mass loss steps are observed in the SIP/PAN blend, which are related to the mass loss characteristics of each component in the blend. The thermal profile of the SIP/PAN blend combines the characteristics of SIP and PAN. Interestingly, at high temperature (500 °C), the SIP/PAN blend has lost less mass (40%) than both PAN (52%) and SIP (65%). Because the FTIR spectrum of the SIP/PAN blend shows the superimposed spectra of SIP and PAN with no new peak formation, as shown in Figure S2, we conclude that there is no chemical interaction between SIP and PAN. It is of course possible that some physical interaction (such as entanglement) can occur between the two polymers.

After successful production of SIP nanofiber membranes using electrospinning, triggered depolymerization of SIP nanofibers upon addition of stimulus was investigated. To confirm the effect on depolymerization of the high surface area of the nanofiber membranes, a comparison was made to the same material in the form of both a cast film and a spin-coated thin film. Figure 3 shows the SIP time release using optical absorption measurements of the solution. Figure 3a shows the appearance of a cast film and a homogeneous PAN/SIP electrospun fiber membrane. It is obvious that the same amount of material (~ 9 mg) can produce much larger sample volume

by electrospinning compared to the cast film, which indicates that electrospun fiber membrane has a surface area much higher than that of the cast film. The spin-coated thin film shown in Figure 3b has the same apparent area and material amount of ~ 9 mg with the electrospun fiber membrane sample but requires a glass substrate to maintain the film formation. When TFA was added to the solution with samples, neither the cast film nor the spin-coated film releases depolymerized SIP noticeably (no color change in solvent), while significant color change from colorless to yellow is observed from the SIP membrane as the depolymerized SIP is released and dissolved into the TFA:DCM mixture. This observation indicates that the SIP fiber membrane provides a faster depolymerization of SIP than film samples because of the fiber membrane's extremely high surface area and porosity. For quantitative analysis, UV-vis spectroscopy was used to measure the absorption spectrum of the solution. The SIP shows a very strong peak at 428 nm (Figure 3c), which is related to the depolymerized SIP oligomers. A significant difference in peak intensity is observed between solutions of SIP fiber membrane and film samples taken 5 min after the addition of TFA. Quantitative analysis of SIP depolymerization as a function of time is shown in Figure 3d. All samples were immersed into DCM only for 2 h, and no noticeable change is observed in all cases, as the triggering condition was not met. However, upon the addition of TFA to the DCM in a volume ratio of 1:20, an abrupt release of depolymerized SIP from the fiber membrane was observed, while the cast and spin-coated film samples show a very slow and gradual depolymerization process. Indeed, for the SIP fiber membrane, $\sim 90\%$ of SIP was depolymerized within 1 h, while only ~ 5 and $\sim 9\%$ of SIP was depolymerized in the cast film and the spin-coated film, respectively, over the same time period.

Triggered depolymerization of SIP was confirmed using gel permeation chromatography (GPC) by measuring the molecular weight (M_n) change before and after depolymerization. The differential refractive index (DRI) technique was used to measure the refractive index of the analyte in solution. Using GPC measurements, it was confirmed that the SIP released from fibers is depolymerized. Figure 4a shows the DRI signal vs elution time in the GPC chromatogram for the PAN/SIP blended fibers immersed in the TFA:DCM solution for different times. The shift of the ~ 42 min peak to ~ 47 – 50 indicates that the SIP polymer size decreased. During depolymerization, the SIP polymer chains break into pieces of different sizes, resulting in the double peak, indicating that the sample is a mixture of species with different sizes. NMR measurement indicates that the released SIP from membranes is depolymerized to SIP oligomers, as shown in Figure S4. For PAN, the peak at ~ 21 min disappears after depolymerization, indicating that PAN was also depolymerized.

As shown in Figure 4b, the molecular weight change is very rapid. The molecular weight of the SIP was reduced from ~ 13 kDa to a final value of ~ 2.5 kDa in 1 min or less. The reduction of M_n reaches a constant low value at 1 min of immersion. \bar{M}_w also reaches a constant value at 5 min, indicating that the depolymerization process is completed. The core and sheath polymers were examined separately in TFA:DCM solution to confirm that the reduced molecular weight is due to SIP in the fiber membrane. Unexpectedly, degraded PAN was also observed in solution, as shown in Figures 4a and 4c. The peak at ~ 27 min is from native PAN, while the peak at ~ 47 min is due to PAN depolymerization. Possibly, the original

peak at ~ 21 min (Figure 4a) shifted to 47 min (Figure 4c) after depolymerization. Although some degradation of the PAN was observed by GPC, the amount of depolymerized PAN should be negligible as SEM observation shows that PAN fiber morphologies are not affected by TFA:DCM (1:20 vol ratio) mixtures as shown in the Supporting Information (Figure S3). The calculated M_n values of the PAN peak near 27 min and degraded PAN near 47 min in GPC measurements are ~ 2.5 MDa and 6 kDa, respectively.

PAN and SIP materials have very different surface properties. PAN is very hygroscopic, absorbing water easily, while the SIP is hydrophobic due to the aromatic rings in the backbone of the polymer chains. The PAN/SIP blended material in a 1:1 wt ratio still exhibits hydrophobic surface properties originating from the SIP molecules. However, upon triggering the depolymerization, a significant amount of SIP is released. At that point, the PAN component becomes dominant, switching the membrane surface from hydrophobic to hygroscopic. This was investigated using static water contact angle (WCA) measurements. Fiber membranes were immersed into either DCM or TFA:DCM solvent for 1 h and then washed with flowing water and dried in a vacuum oven. WCA on a PAN/SIP blended fiber membrane without depolymerization (Figure 5a)

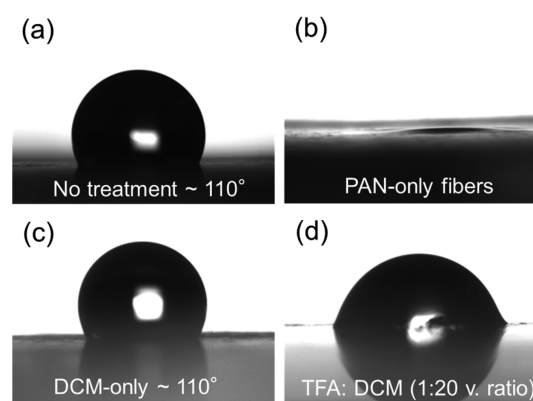


Figure 5. Comparison of surface properties obtained using water contact angle measurements on (a) SIP/PAN blended nanofiber membrane; (b) PAN-only nanofiber membrane; SIP/PAN nanofiber membrane after 1 h immersion into (c) DCM-only (nontriggering) solvent, and into (d) TFA:DCM (1:20 vol ratio) triggering solvent (water contact measurements on spin-coated smooth thin films (PAN, SIP, and SIP/PAN blend films) are shown in Figure S5)).

is $\sim 110^\circ$, while WCA on a pure PAN fiber membrane cannot be measured because the water droplet is rapidly absorbed into the membrane (Figure 5b). When the PAN/SIP membrane was treated with DCM only, no change in the WCA was observed, as shown in Figure 5c. However, after depolymerizing the SIP sheath in TFA:DCM, the WCA on the membrane surface was significantly reduced from its initial value (Figure 5d), and the water droplet was gradually absorbed into the membrane within one minute. Therefore, using the PAN/SIP blend as a sheath layer in the coaxial fiber can utilize the transition of surface properties to provide a significant effect on the release kinetics of core components. Also, the WCA on the SIP/PAN thin film ($\sim 70^\circ$) is closer to that on the SIP thin film ($\sim 79^\circ$) than to the WCA on the PAN-only thin film ($\sim 50^\circ$), as shown in Figure S5. All water contact angle measurements were carried out on the FTA200 dynamic contact angle and surface tension

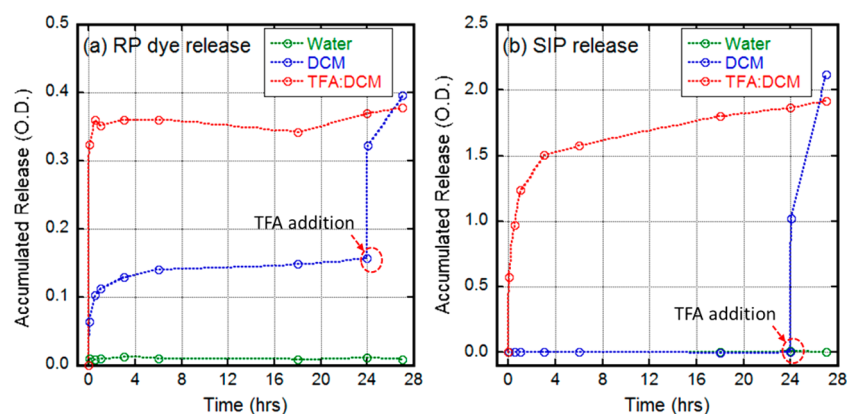


Figure 6. Time dependence of release from coaxial fibers with PAN/SIP sheath and PVP core with RP dye molecules: (a) RP dye release profile from core and (b) depolymerized SIP release profile from sheath in either water, DCM-only solvent, or TFA:DCM (1:20 vol. ratio) solvent. After 24 h, TFA was added to the case of DCM-only solvent in the same volume ratio of 1:20.

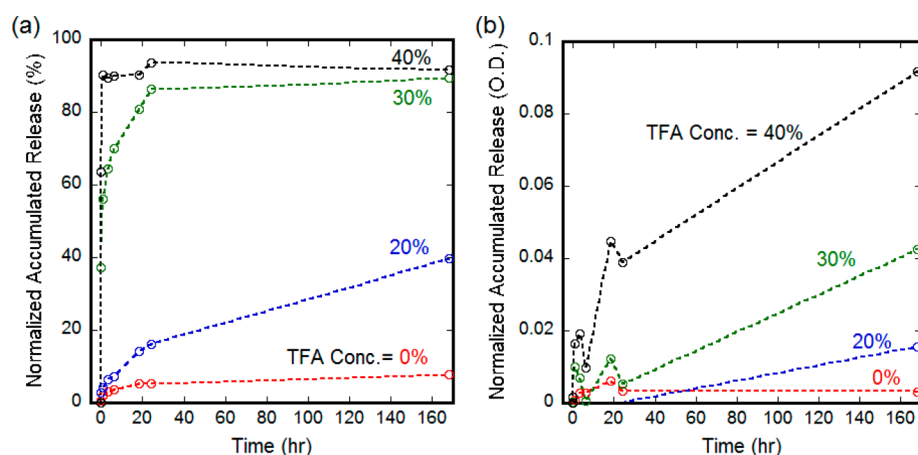


Figure 7. Time dependent release characteristics from coaxial SIP fibers in aqueous solutions of TFA: (a) KAB dye release from the core and (b) SIP release from the sheath.

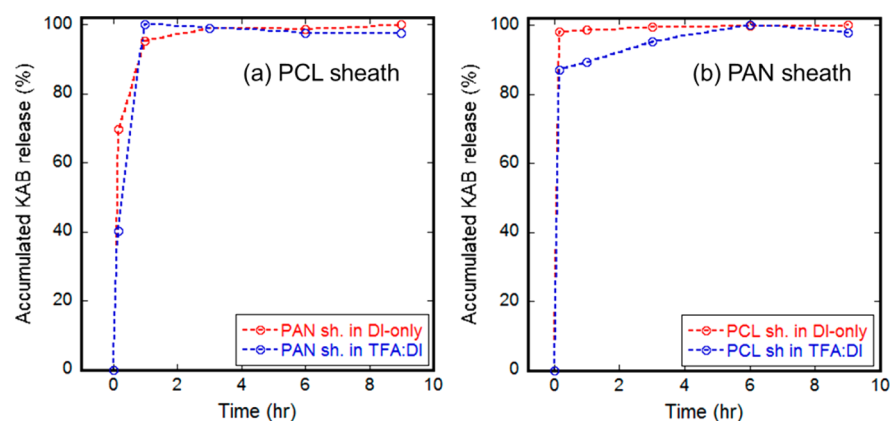


Figure 8. KAB release profiles from coaxial fibers without SIP: (a) coaxial fiber with PCL sheath and PVP/KAB core and (b) coaxial fibers with PAN sheath and PVP/KAB core.

analyzer system (First Ten Angstroms, Portsmouth, VA), placing 2 μL water droplets on sample surfaces.

To investigate the triggered release of functional material, coaxial fiber membranes were made using a PAN/SIP (1:1) blend for the sheath and PVP with a dye (RP (Rhodamine 640 perchlorate) or KAB (Keyacid blue)) for the core. The release kinetics of the dyes were examined quantitatively using UV–vis spectroscopy, as shown in Figure 6. No noticeable release was

observed in water due to the strong hydrophobic properties of the PAN/SIP sheath encapsulating the PVP/RP core. However, under triggering conditions with TFA:DCM (1:20) solvent, the encapsulated RP dye in the core was released swiftly (Figure 6a), reaching $\sim 100\%$ release within 1 h. The depolymerized SIP was released quickly within the first 3 h and then released more gradually (Figure 6b). Although the coaxial fibers have some initial dye “burst” release in DCM, a dramatic triggered

release is observed upon applying TFA stimulus. The amount of dye released under nontriggering conditions was saturated after the initial burst release. However, as shown in Figure 6a, the majority of the dye in the fiber core was abruptly released after adding TFA to DCM solvent, which is the triggering condition for SIP depolymerization.

The triggered release of functional molecules in aqueous media is a key requirement for many applications. Therefore, the release characteristics from SIP coaxial fibers in aqueous solution were also investigated. Because the released dye was degraded in TFA:DI mixtures, we normalized the released KAB and SIP considering the degraded KAB intensity, as shown in the Supporting Information (Figure S6). As shown in Figure 7a, in the case of pure aqueous solution, only a minimal dye release from the core was observed even after 1 week. However, at 30 and 40% TFA concentrations, almost 100% of encapsulated KAB dye in core was released within 1 day. Interestingly, at 20% TFA concentration, continuously increasing (sustained) release from the core was observed for the 1 week period. The depolymerized SIP release from the sheath shows a trend (Figure 7b) similar to that of the KAB release from core. The released SIP represents less than 5% of total SIP amount incorporated into fibers because depolymerized SIP does not dissolve well into an aqueous environment due to the hydrophobic nature of the aromatic ring on the SIP backbone.

To confirm the unique effect of SIP triggered depolymerization, coaxial fibers with different sheath material (without SIP) were tested. Shown in Figure 8 are release characteristics from coaxial fiber membranes with either PCL or PAN sheath, and PVP/KAB core. For this comparison, membranes were immersed into either DI-only solution or a TFA:DI mixture at ~3:7 volume ratio. Unlike SIP coaxial fibers, these coaxial fibers showed an abrupt release of core material, and no triggering behavior was observed when comparing a DI-only solution and a TFA:DI mixture. The PCL sheath material was severely damaged in the TFA:DI mixture, and even slightly slower release of KAB dye was observed due to the lower solubility of PVP/KAB core in TFA:DI mixtures (Figure 8a). PAN is very hygroscopic material and therefore results in abrupt release of core material in both conditions (Figure 8b). These results indicate that triggered release kinetics shown in Figures 6 and 7 are provided by the addition of SIP in sheath layer.

CONCLUSIONS

Considering these results, the authors believe that this work represents the first nanofiber membranes made of a stimuli-responsive self-immolative polymer successfully produced by (coaxial) electrospinning. In particular, core–sheath structured fibers incorporating SIP in the sheath were carefully evaluated to demonstrate the stimulus-triggered release of the encapsulated functional core components. Unlike microcapsules, electrospun nanofiber membranes are self-standing nanostructures with extremely high surface area and porosity, properties very beneficial for stimuli-responsive applications. The demonstration that electrospun SIP membranes can be obtained with highly sensitive and responsive depolymerization to the external stimuli has opened the path to many important applications. While the triggered burst release is important for many applications such as sensors and catalysts, a controlled triggered release will also provide versatility and the ability to use this approach for many other important areas, including

drug delivery, environmental, and agricultural applications. In Figure 9, a triaxial fiber structure is illustrated, which includes

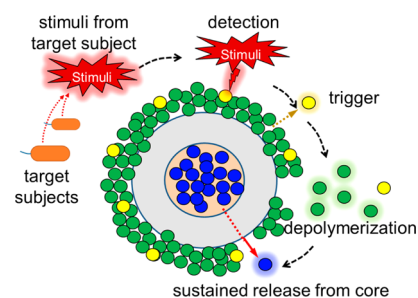


Figure 9. Concept diagram: cross section of triaxial fiber with a self-immolative sheath, hydrophobic intermediate layer, and encapsulated core material. This diagram shows possibly the best combination of material and structure to enable the triggered sustained release by external stimuli (yellow circle, head molecules of SIP; green circle, SIP monomers; blue circle, encapsulated molecules).

an intermediate layer between the SIP sheath and the encapsulated core. This enables the triggered and sustained release of core material upon SIP depolymerization, which can be manipulated by selecting the material and adjusting the thickness of the intermediate layer.

Preparing SIPs with higher molecular weights should result in important future improvements. The currently utilized SIPs have a small molecular weight that cannot produce a solution with sufficient viscosity for a robust electrospinning process in pure form even at very high concentrations. While coaxial fibers with an SIP-only sheath were produced, the flow rate was very limited, and it was very difficult to maintain a stable electrospinning process, which is required to fully encapsulate the core material within coaxial fibers. SIP with high molecular weight enables the formation of coaxial fibers with pure SIP sheath encapsulating core materials. Applying polymers that are (a) inherently more biocompatible and (b) triggered by more benign stimuli will be another future improvement. Various SIPs, including nontoxic SIPs, are in the process of being developed, which can be triggered by various stimuli. On the basis of the results demonstrated in this report, it is clear that SIP can be easily incorporated into nanofibers and nanofiber membranes using electrospinning, showing the remarkable and significant increase in rate of release from electrospun polymers rather than bulk monoliths. It is hoped that this can have a positive impact on smart material development for various applications such as sensors and drug delivery.

ASSOCIATED CONTENT

Supporting Information

The Supporting Information is available free of charge on the ACS Publications website at DOI: 10.1021/acsami.6b16501.

Figure S1, thermal properties of PAN-only, SIP-only, and SIP/PAN blend; Figure S2, FTIR spectrum of PAN, SIP, and SIP/PAN blend materials; Figure S3, SEM observations; Figure S4, NMR spectra; Figure S5, water contact angle measurements, Figure S6; KAB dye degradation in TFA:DI water mixtures (PDF)

AUTHOR INFORMATION

Corresponding Author

*E-mail: a.steckl@uc.edu.

ORCID 

Xinjun Yu: 0000-0002-4324-7332

Andrew J. Steckl: 0000-0002-1868-4442

Notes

The authors declare no competing financial interest.

ACKNOWLEDGMENTS

D.H. and A.J.S. were generously supported by the Natick Soldier Research Development and Engineering Center (NSRDEC) under Grant W911NF-11-D-0001. The authors would like to acknowledge many useful discussions with Dr. Shaun Filocamo and administrative support from Michael Dion at NSRDEC. X.Y. and N.A. acknowledge support from the University of Cincinnati.

REFERENCES

- (1) Stuart, M. A. C.; Huck, W. T. S.; Genzer, J.; Muller, M.; Ober, C.; Stamm, M.; Sukhorukov, G. B.; Szleifer, I.; Tsukruk, V. V.; Urban, M.; Winnik, F.; Zauscher, S.; Luzinov, I.; Minko, S. Emerging Applications of Stimuli-Responsive Polymer Materials. *Nat. Mater.* **2010**, *9* (2), 101–113.
- (2) Cabane, E.; Zhang, X.; Langowska, K.; Palivan, C. G.; Meier, W. Stimuli-Responsive Polymers and Their Applications in Nanomedicine. *Biointerphases* **2012**, *7* (1), 1–27.
- (3) Huang, C.; Soenen, S. J.; Rejman, J.; Lucas, B.; Braeckmans, K.; Demeester, J.; De Smedt, S. C. Stimuli-Responsive Electrospun Fibers and Their Applications. *Chem. Soc. Rev.* **2011**, *40* (5), 2417–2434.
- (4) Sagi, A.; Weinstain, R.; Karton, N.; Shabat, D. Self-Immolative Polymers. *J. Am. Chem. Soc.* **2008**, *130* (16), 5434–5435.
- (5) Kaitz, J. A.; Lee, O. P.; Moore, J. S. Depolymerizable Polymers: Preparation, Applications, and Future Outlook. *MRS Commun.* **2015**, *5* (02), 191–204.
- (6) Peterson, G. I.; Larsen, M. B.; Boydston, A. J. Controlled Depolymerization: Stimuli-Responsive Self-Immolative Polymers. *Macromolecules* **2012**, *45* (18), 7317–7328.
- (7) Wang, H.-C.; Zhang, Y.; Possanza, C. M.; Zimmerman, S. C.; Cheng, J.; Moore, J. S.; Harris, K.; Katz, J. S. Trigger Chemistries for Better Industrial Formulations. *ACS Appl. Mater. Interfaces* **2015**, *7* (12), 6369–6382.
- (8) Amir, R. J.; Danieli, E.; Shabat, D. Receiver–Amplifier, Self-Immolative Dendritic Device. *Chem. - Eur. J.* **2007**, *13* (3), 812–821.
- (9) Sella, E.; Shabat, D. Self-Immolative Dendritic Probe for Direct Detection of Triacetone Triperoxide. *Chem. Commun.* **2008**, *44*, 5701–5703.
- (10) Weinstain, R.; Sagi, A.; Karton, N.; Shabat, D. Self-Immolative Comb-Polymers: Multiple-Release of Side-Reporters by a Single Stimulus Event. *Chem. - Eur. J.* **2008**, *14* (23), 6857–6861.
- (11) Esser-Kahn, A. P.; Sottos, N. R.; White, S. R.; Moore, J. S. Programmable Microcapsules from Self-Immolative Polymers. *J. Am. Chem. Soc.* **2010**, *132* (30), 10266–10268.
- (12) DiLauro, A. M.; Abbaspourrad, A.; Weitz, D. A.; Phillips, S. T. Stimuli-Responsive Core–Shell Microcapsules with Tunable Rates of Release by Using a Depolymerizable Poly(phthalaldehyde) Membrane. *Macromolecules* **2013**, *46* (9), 3309–3313.
- (13) Fan, B.; Trant, J. F.; Wong, A. D.; Gillies, E. R. Polyglyoxylates: A Versatile Class of Triggerable Self-Immolative Polymers from Readily Accessible Monomers. *J. Am. Chem. Soc.* **2014**, *136* (28), 10116–10123.
- (14) Tong, R.; Kohane, D. S. New Strategies in Cancer Nanomedicine. *Annu. Rev. Pharmacol. Toxicol.* **2016**, *56* (1), 41–57.
- (15) Kim, J. S.; Reneker, D. H. Polybenzimidazole Nanofiber Produced by Electrospinning. *Polym. Eng. Sci.* **1999**, *39* (5), 849–854.
- (16) Li, D.; Xia, Y. N. Electrospinning of Nanofibers: Reinventing the Wheel? *Adv. Mater.* **2004**, *16* (14), 1151–1170.
- (17) Wang, Z.-G.; Wan, L.-S.; Liu, Z.-M.; Huang, X.-J.; Xu, Z.-K. Enzyme Immobilization on Electrospun Polymer Nanofibers: An Overview. *J. Mol. Catal. B: Enzym.* **2009**, *56* (4), 189–195.
- (18) Han, D.; Filocamo, S.; Kirby, R.; Steckl, A. J. Deactivating Chemical Agents using Enzyme-coated Nanofibers Formed by Electrospinning. *ACS Appl. Mater. Interfaces* **2011**, *3* (12), 4633–4639.
- (19) Han, D.; Steckl, A. J. Superhydrophobic and Oleophobic Fibers by Coaxial Electrospinning. *Langmuir* **2009**, *25*, 9454–9462.
- (20) Han, D.; Steckl, A. J. Triaxial Electrospun Nanofiber Membranes for Controlled Dual Release of Functional Molecules. *ACS Appl. Mater. Interfaces* **2013**, *5* (16), 8241–8245.
- (21) Yarin, A. L. Coaxial Electrospinning and Emulsion Electrospinning of Core-Shell Fibers. *Polym. Adv. Technol.* **2011**, *22* (3), 310–317.
- (22) Moghe, A. K.; Gupta, B. S. Co-axial Electrospinning for Nanofiber Structures: Preparation and Applications. *Polym. Rev.* **2008**, *48*, 353–377.
- (23) Yu, J. H.; Fridrikh, S. V.; Rutledge, G. C. Production of Submicrometer Diameter Fibers by Two-Fluid Electrospinning. *Adv. Mater.* **2004**, *16* (17), 1562–1566.
- (24) McBride, R. A.; Gillies, E. R. Kinetics of Self-Immolative Degradation in a Linear Polymeric System: Demonstrating the Effect of Chain Length. *Macromolecules* **2013**, *46* (13), 5157–5166.
- (25) Song, C.-C.; Ji, R.; Du, F.-S.; Li, Z.-C. Oxidation-Responsive Poly(amino ester)s Containing Arylboronic Ester and Self-Immolative Motif: Synthesis and Degradation Study. *Macromolecules* **2013**, *46* (21), 8416–8425.
- (26) Zelzer, M.; Todd, S. J.; Hirst, A. R.; McDonald, T. O.; Ulijn, R. V. Enzyme Responsive Materials: Design Strategies and Future Developments. *Biomater. Sci.* **2013**, *1* (1), 11–39.
- (27) Weinstain, R.; Baran, P. S.; Shabat, D. Activity-Linked Labeling of Enzymes by Self-Immolative Polymers. *Bioconjugate Chem.* **2009**, *20* (9), 1783–1791.
- (28) Zhao, C.; Nie, S.; Tang, M.; Sun, S. Polymeric pH-Sensitive Membranes—A Review. *Prog. Polym. Sci.* **2011**, *36* (11), 1499–1520.
- (29) Wang, Z.; Sun, J.; Jia, X. Self-Immolative Nanoparticles Triggered by Hydrogen Peroxide and pH. *J. Polym. Sci., Part A: Polym. Chem.* **2014**, *52* (14), 1962–1969.
- (30) Pasparakis, G.; Manouras, T.; Argitis, P.; Vamvakaki, M. Photodegradable Polymers for Biotechnological Applications. *Macromol. Rapid Commun.* **2012**, *33* (3), 183–198.